# Precision Measurement of Electrical Characteristics of Quartz-Crystal Units*

W. D. GEORGE†, ASSOCIATE, IRE, M. C. SELBY†, SENIOR MEMBER, IRE, AND R. SCOLNIK†

**Summary—Extensive manufacture and use of quartz-crystal units for radio communication, instrumentation, control, and detection purposes was responsible for new investigations to improve all phases of piezoelectric units and devices. A small part of the total work included development of circuit arrangements and instruments for accurately measuring the electrical constants of crystal units. This paper describes precision methods of high-frequency radio measurements as used successfully on quartz-crystal units and applicable to other types of units having $Q$'s and impedance ranges up to several million or higher.**

## I. Introduction

As a result of the enormous demand for quartz-crystal units in the recent war, many new methods of production, measurement, and testing were studied and put to use. Precise measurements of many characteristics of crystal units were made, but data concerning the dynamic electric impedance were supplied largely in an arbitrary and indirect manner.[1,2]

The electrical characteristics of a crystal unit, i.e., the impedance, the equivalent reactance, and the equivalent resistance at any point of operation may be measured and specified entirely apart from any external circuit with which the crystal unit is used.[3–5] From these data the behavior of a crystal unit in any specific external circuit whose characteristics are known may be predicted. Although the great advantages of using this kind of data as the basis for a standardization of crystal units are described at length by others,[3,5] it may briefly be noted that this application would eliminate the multitude of comparison test sets and the associated problems of calibration and maintenance required by today's indirect methods of specification, and should lead to more exact methods of measurement and performance rating in terms of those parameters likely to be most useful to the radio and electronics design engineer.

This paper reviews means of expressing the equivalent electrical circuit of a quartz-crystal unit. It describes measurement methods and techniques in which a generator of continuously adjustable frequency of stability comparable to that of a crystal unit permits the use of such laboratory instruments as rf bridges and $Q$ meters to determine the crystal unit's electrical parameters. It shows how the techniques may be used for exploring secondary responses in a crystal unit to determine its usefulness as an element in filter circuits and to investigate causes of instability in oscillator circuits. The data are presented in simple graphical form favoring differentiation between a "normal" crystal unit and one remaining constant under limited conditions. Finally, correlation is shown between data based on the more fundamental crystal-unit characteristics and data derived from the more familiar "activity" and "stability" of a particular oscillator.

This work was done in connection with development of precision laboratory methods of measuring high-$Q$ components.

## II. Equivalent Circuit Representing a Normal Mode of Vibration of a Quartz-Crystal Unit

Piezoelectric crystals were introduced into the radio-frequency field to meet the need for a resonant circuit (series or parallel) having constant parameters and high $Q$. A fundamental requirement was that the crystal unit be the electrical equivalent of a single resonant (or antiresonant) circuit. The unit that for practical purposes meets this requirement is called a normal one. Crystal units with interfering responses, or closely spaced multiple responses, are apparently equivalent to electrical circuit meshes with a number of mutually coupled resonant circuits. These are more complex units, and should be treated separately.

The equivalent circuit of a normal crystal unit is shown in Fig. 1(a). It has one resonant frequency $f_r$ and one antiresonant frequency $f_a$ for any particular value of shunting capacitance $C_t$. The impedance across its terminals $R_p$ is illustrated by means of the susceptance with reactance diagrams of Fig. 1(c) and (d). $R_s$ is small as compared with $\omega L$, and can be neglected in these diagrams.

The susceptance $B_{abc}$ of the $L_1$, $C_1$ series branch is added to the susceptance $B_t$ of the shunt capacitance $C_t$. $C_t$ is the total shunt capacitance across the crystal plate, and is usually designated as $C_0$ when the capacitance external to the crystal unit is zero. The resultant

* Decimal classification: R214.211. Original manuscript received by the Institute, November 21, 1946; revised manuscript received, March 5, 1948. Presented, 1946 Winter Technical Meeting, January 26, 1946, New York, N. Y.

† Central Radio Propagation Laboratory, National Bureau of Standards, Washington 25, D. C.

[1] G. M. Thurston, "A crystal test set," *Bell Labs. Rec.*, vol. 22, pp. 477–480; 1944.

[2] W. E. McNatt, "Test set for quartz crystals," *Electronics*, vol. 18, pp. 113–115; April, 1945.

[3] Karl S. Van Dyke, "The standardization of quartz-crystal units, Proc. I.R.E., vol. 33, pp. 15–20; January, 1945.

[4] Geoffrey Builder, "A note on the determination of the equivalent electrical constants of a quartz-crystal resonator," *A.W.A. Tech. Rev.*, vol. 5, pp. 41–45; April, 1940.

[5] C. W. Harrison, "The measurement of the performance index of quartz plates," *Bell Sys. Tech. Jour.*, vol. 24, pp. 217–252; April, 1945.

$B_e$ is obtained in Fig. 1(c) as the resultant termination reactance $X_e$ in Fig. 1(d). It is evident from the diagram that, as $C_t$ is increased in value, the slope of $B_t$ will increase, and $f_a$ will approach $f_r$. It is also apparent that $X_e$ is positive between $f_r$ and $f_a$. The equivalent circuit at frequencies in this range is, therefore, as shown in Fig. 1(b), where $R_e$ is the resistive component including the effect of the series resistance $R_s$ and all other losses of the unit.

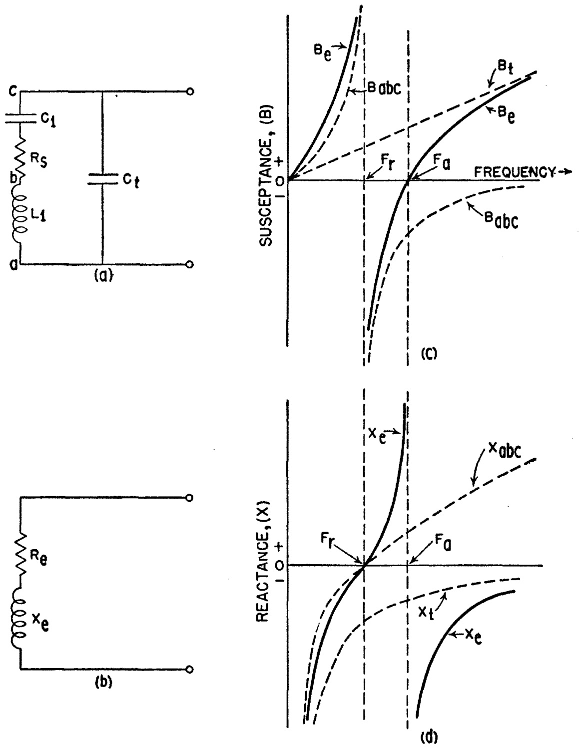


Fig. 1—(a) Equivalent circuit of a quartz-crystal unit. (b) Effective impedance of a crystal unit between $f_r$ and $f_a$. (c) Susceptance diagram of a crystal unit. (d) Reactance diagram of a crystal unit.

When such a circuit is tuned to antiresonance with an external capacitor, the termination impedance is resistive, and is equal to

$$R_p = Q_e X_e = \frac{X_e^2}{R_e}. \qquad (1)$$

The termination impedance of the equivalent circuit of Fig. 1(b) (often referred to as the Performance Index, or *PI*) may also be expressed in terms of the shunt capacitance and the series resistance, as follows:

At any antiresonant frequency $f_a$ (where $f_a > f_r$), the termination impedance is, for small values of $R_s$, equal to that of a tapped antiresonant circuit, and is resistive; namely,

$$Z_p = R_p = Z_x \frac{C_1^2}{(C_1 + C_t)^2}$$

where

$$Z_x = Q_x \frac{1}{\omega_a C_e} = \frac{1}{R_s(\omega_a C_e)^2}.$$

$Q_x$ is the $Q$ of the antiresonant circuit, and

$$C_e = \frac{C_1 C_t}{C_1 + C_t}.$$

Now,

$$R_p \doteq Z_x \frac{C_e^2}{C_t^2} = \frac{1}{R_s(\omega_a C_t)^2} = \frac{X_t^2}{R_s}. \qquad (2)$$

And, from (1) and (2),

$$\frac{X_t^2}{R_s} \doteq \frac{X_e^2}{R_e}. \qquad (3)$$

$R_p$ may be plotted versus $C_t$ as an independent parameter on log-log co-ordinate paper in the form of a straight line with a negative 2-to-1 slope. This follows from (2), since

$$\log R_p = \log \left[\frac{1}{\omega^2 R_s C_t^2}\right] = \log \left[\frac{1}{\omega^2 R_s}\right] - 2 \log C_t.$$

$R_s$ is assumed constant and the percentage change in $\omega$ with $C_t$ negligible. Experimental evidence shown later supports these assumptions. Hence,

$$\log R_p = K_1 - 2 \log C_t. \qquad (4)$$

Similarly, the antiresonant frequency increments $(f_a - f_r)$ may be plotted on log-log paper as a straight-line function of $C_t$ with a negative 1-to-1 slope. This may be shown as follows (see Fig. 1(a)):

$$\omega_r^2 = \frac{1}{L_1 C_1}. \qquad (5)$$

The antiresonance frequency is determined from the interrelation:

$$\omega_a^2 = \frac{1}{L_1 \dfrac{C_1 C_t}{C_1 + C_t}} = \frac{C_1 + C_t}{L_1 C_1 C_t}.$$

From this and (5),

$$\frac{\omega_a^2}{\omega_r^2} = \frac{f_a^2}{f_r^2} = \frac{(C_1 + C_t)C_1}{C_1 C_t} = 1 + \frac{C_1}{C_t}$$

or

$$\frac{C_1}{C_t} = \frac{f_a^2}{f_r^2} - 1 = \frac{(f_a + f_r)(f_a - f_r)}{f_r^2}.$$

For practical purposes, $f_a + f_r = 2f_r$.
Hence,

$$(f_a - f_r) \doteq \frac{1}{2} \frac{f_r C_1}{C_t} \qquad (6)$$

or

$$\log (f_a - f_r) \doteq \log (\tfrac{1}{2} f_r C_1) - \log C_t.$$

Since $f_r$ and $C_1$ are constant,

$$\log (f_a - f_r) \doteq K_2 - \log C_t. \tag{7}$$

These straight-line characteristics ((4), (7)) of normal crystal units are demonstrated in Figs. 2, 3, and 4. Slopes of 2-to-1 and 1-to-1 were drawn for the straight-line sections in the figures. The position of each measured point shows how closely the theoretical curves are followed. Curvatures at high $R_p$ values were caused by holder losses, as evidenced by the same characteristics measured, and plotted in Fig. 5, with the crystal removed from the holder.

It might seem at this time as if a single point on each of these $R_p$ and $(f_a - f_r)$ versus $C_t$ curves, through which the engineer could draw the appropriate 2-to-1 and 1-to-1 lines, would convey sufficient data for design purposes. And this could almost be done if the crystal unit in question were known to be normal, and if the

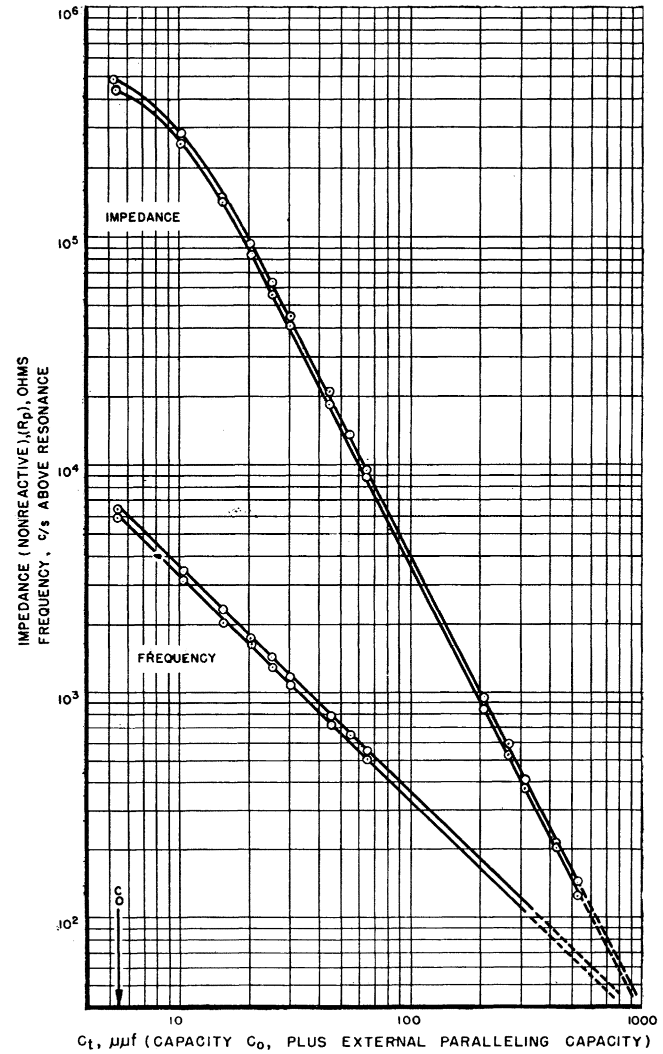


Fig. 2—Electrical characteristics of two 8.7-Mc wire-mounted crystal units with metal-film electrodes. These exhibit the 2-to-1 and 1-to-1 slopes derived from theory.

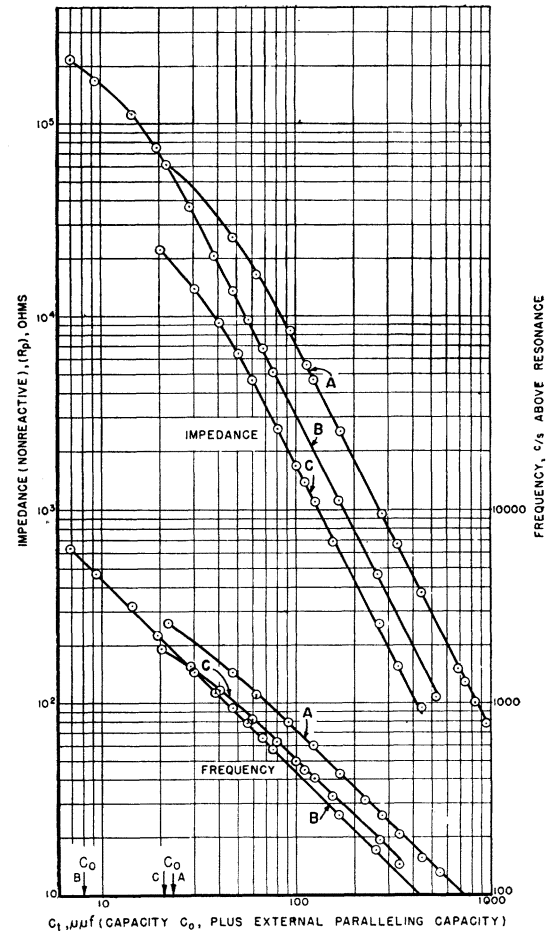


Fig. 3—Electrical characteristics of "normal" crystal units of different physical construction. (a) CR-1 type; air-gap, pressure-mounted. (b) FT-243 type; metal-film, spring-clip mounting. (c) FT-243 type; air-gap, pressure-mounted.

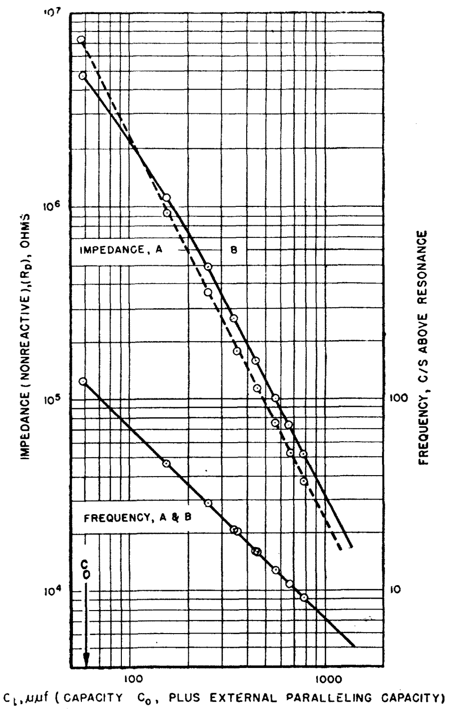


Fig. 4—Electrical characteristics of two different 100-kc quartz crystal units; *GT*-cut, metal-film electrodes, wire-mounted crystal. Unit A had a low-loss holder.

engineer were supplied with such additional data as the values of $C_0$ and either $f_r$ or $f_a$ at $C_0$. Still lacking, however, would be the effect of holder losses, and the frequency spectrum of the crystal unit showing the magnitude and disposition of secondary responses and data on parameter variation with temperature.

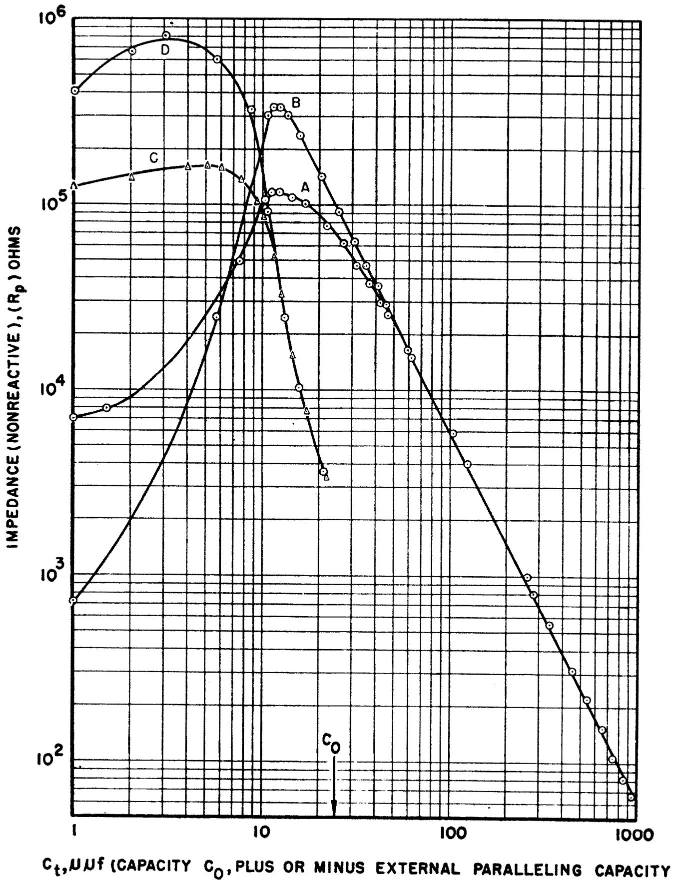


Fig. 5—Impedance measurements of the fundamental and adjacent responses on both sides of antiresonance of an air-gap, pressure-mounted crystal unit. The effect of holder losses on the high $R_p$ values of a crystal unit is shown. Fundamental response: (a) Lossy holder. (b) Low-loss holder. Secondary response: (c) Lossy holder. (d) Low-loss holder.

## III. Measurement Methods

Those parameters investigated in these measurements, which have not yet been defined and are not presented in Fig. 1, are:

$\Delta C_t$ = an increment of $C_t$

$\Delta f = f_a - f_r$

$R_h$ = resistance shunting the quartz crystal (equivalent to holder losses)

$Q_e = X_e/R_e$ = the effective $Q$ of the crystal unit

$Q_x = (2\pi f L_1/R_s) = (1/2\pi f C_1 R_s)$ by definition, where $f$ is the nominal frequency of the crystal unit. is usually referred to as the $Q$ of the crystal.

Some useful expressions of parameters in terms of directly measurable quantities are derived as follows:

$$C_1 \doteq \frac{2\Delta f C_t}{f_r} = \text{equation (6) rearranged.} \tag{8}$$

$$Q_x = \frac{1}{4\pi\Delta f C_t R_s} \text{ from definition of } Q_x \text{ and (8); noting that,} \tag{9}$$

since $\Delta f \ll f_r$ any frequency between $f_a$ and $f_r$ can be used.

Measurements of $f_a$ (to determine $\Delta f$) are usually made at $C_t = C_0$. Then,

$$Q_x = \frac{1}{4\pi\Delta f C_0 R_s} \tag{10}$$

$$L_1 = \frac{1}{(2\pi f_r)^2 C_1}. \tag{11}$$

The effect of holder losses reduce $R_p$ to

$$R_p' = \frac{R_h R_p}{R_h + R_p}. \tag{12}$$

### A. Q-Meter Measurements of Quartz-Crystal Unit Characteristics

The well-known $Q$-meter principle makes use of an antiresonant circuit arrangement as shown in the table (Fig. 6). For our purposes, constant rf voltage was applied directly to the 0.04-ohm resistance element in the $Q$-meter tank with the $Q$ meter's internal oscillator disconnected by leaving the band switch in an intermediate position.

$L_Q$, $C_Q$ (Fig. 6) is tuned for antiresonance at the frequency at which $X_e$, $R_e$ are to be measured. The crystal unit is connected in parallel with $C_Q$. Now the latter must be readjusted by $\Delta C_Q$ to restore the antiresonance at the $Q$-meter tank, and

$$X_e = \frac{1}{\omega\Delta C_Q}. \tag{13}$$

The voltage across the antiresonance tank is a measure of the $Q$ of the circuit. Connecting the crystal unit in parallel with the tank reduces the original $Q$ as a result of the shunt effect of $R_e$. From the two values of $Q$,

$$R_e = \frac{1.59 \times 10^8\left(\frac{C_{Q1}}{C_{Q2}} Q_1 - Q_2\right)}{f C_{Q1} Q_1 Q_2} \tag{14}$$

where $C_{Q1}$ is the capacitance, in micromicrofarads, required to tune the $Q$-meter tank without the crystal unit, but at the crystal frequency; $C_{Q2}$ is the capacitance, in micromicrofarads, required to tune the $Q$-meter tank with the crystal unit in parallel with it; $Q_1$ is the original $Q$ of the tank; $Q_2$ is the reduced $Q$ of the tank; and $f$ is the nominal frequency of the crystal unit in kc.

| PARAMETER | RANGE | INSTRUMENT | CIRCUIT ARRANGEMENT (FUNDAMENTAL SCHEMATIC) | PROCEDURE | PRECAUTIONS | ACCURACY, CONSERVATIVE ESTIMATE |
|---|---|---|---|---|---|---|
| STATIC CAPACITY $C_0$, AND PARALLELING CAPACITY $\Delta C_t$ | 0 TO 30 $\mu\mu f$ | "Q" METER | SEE $f_a$ | CALIBRATE $C_Q$ VS. DIAL SETTING. $C_0 = C_{Q_1} - C_{Q_2}$ | MEASURE $C_0$ AT r.f. FOR WHICH CRYSTAL IS INACTIVE | ± 0.1 $\mu\mu f$ |
| | 30 TO 150 $\mu\mu f$ | | | | | ± 0.2 $\mu\mu f$ |
| | 150 TO 2000 $\mu\mu f$ | | | | POSITION AND SHIELDING OF CRYSTAL UNIT IS IMPORTANT | ± 5 $\mu\mu f$ |
| | 100 TO 1100 $\mu\mu f$ | TWIN-T IMPEDANCE-MEASURING CIRCUIT | SEE $R_p$ | CALIBRATE CAPACITANCE DIAL | | ± 2 $\mu\mu f$ |
| SERIES-RESONANCE FREQUENCY, $f_r$ | "Q" METER | "Q" METER | 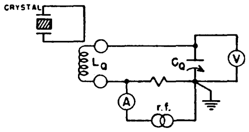 | ADJUST $L_QC_Q$ FOR MAXIMUM V. ADJUST r.f. FOR MINIMUM V. | USE SHORTED TERMINALS OR SMALLEST LOOP FOR INDUCTIVE COUPLING TO CRYSTAL UNIT | ± 1.5 IN $10^6$ |
| | R-F BRIDGE | R-F BRIDGE | SEE $R_s$ AND $R_s$ (HIGH LEVEL) | ADJUST r. f., AND RESISTANCE ARM OF BRIDGE FOR BALANCE | SHIELD WELL. NO F.M. IN OUTPUT OF r-f GENERATOR | ± 1.5 IN $10^6$ |
| ANTIRESONANCE FREQUENCY, $f_a$ | "Q" METER | "Q" METER | 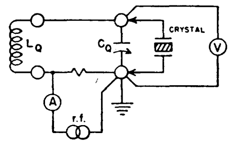 | TUNE "Q" METER TO $f_r$. PLACE CRYSTAL UNIT IN PARALLEL WITH $C_Q$. INCREASE r.f. FOR MAX. V. REMOVE CRYSTAL UNIT AND RETUNE "Q" METER. REPLACE CRYSTAL UNIT AND READJUST r.f. FOR MAX V. | FOR MAXIMUM PRECISION ADJUST $C_Q$ FOR MAX. V. USE LARGE L/C RATIO IN "Q" METER | ± 2.5 IN $10^6$ |
| | TWIN-T CIRCUIT | TWIN-T CIRCUIT | SEE $R_p$ (LOW LEVEL) | ADJUST r. f., AND $C_Q$ ARM OF BRIDGE FOR BALANCE | SHIELD WELL | ± 2.5 IN $10^6$ |
| EQUIVALENT SERIES RESISTANCE $R_e$; AND REACTANCE, $X_e$ | 0 TO 1000 OHMS | R-F BRIDGE | SEE $R_s$ | ROUTINE | SHIELD WELL. USE LOW r-f INPUT TO BRIDGE | ± 0.2 OHMS ± 2% |
| | 0 TO 500 OHMS (AT 10 Mc.) | | | | | ± 1 OHM ± 1% |
| ANTIRESONANCE IMPEDANCE, $R_p$ (LOW LEVEL) | 5000 TO 10,000 OHMS | "Q" METER | SEE $f_a$ | SUBSTITUTION METHOD ADJUST r.f. FOR MAXIMUM V. AT EACH $\Delta C_t$ | FOR MAXIMUM PRECISION ADJUST $C_Q$ FOR MAX. V. | ± 5% OR BETTER |
| | 10,000 TO 100,000 OHMS | | | | | ± 2% |
| | 100,000 TO 5,000,000 OHMS | | | | | ± 5% OR BETTER |
| | 1000 TO 18,000 OHMS | TWIN-T CIRCUIT | 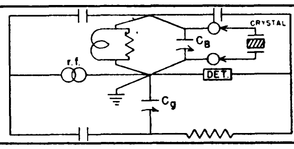 | ROUTINE | SHIELD WELL. USE LOW r-f INPUT TO BRIDGE | ± 2.5% |
| | 0 TO 1000 OHMS | R-F BRIDGE | 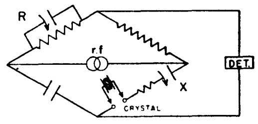 | ADJUST r.f., AND RESISTANCE ARM OF BRIDGE FOR BALANCE WITH CALIBRATED SILVER-MICA CONDENSERS IN PARALLEL WITH CRYSTAL UNIT | SHIELD WELL. USE LOW r-f INPUT TO BRIDGE. NO F.M. IN OUTPUT OF r-f GENERATOR | ± 0.1 OHMS ± 1.5% |
| $R_p$ (HIGH LEVEL) | 1000 TO 100,000 OHMS | SPECIAL HIGH LEVEL "Q" METER | 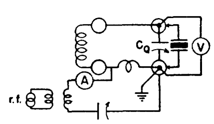 | SUBSTITUTION METHOD. USE 1 TO 5 WATT r-f INPUT | PERMIT CRYSTAL UNIT TO REACH TEMPERATURE EQUILIBRIUM | ± 5% |
| SERIES-RESONANCE RESISTANCE, $R_s$ | 0 TO 1000 OHMS | R-F BRIDGE | SEE $R_p$ (LOW LEVEL) | SEE $f_r$ | SEE $f_r$ | ± 0.1 OHM ± 1% |
| | 1000 TO 10,000 OHMS | "Q" METER | SEE $f_a$ | SUBSTITUTION METHOD | USE GOOD $L_Q$ COILS AND LOW $L_Q/C_Q$ RATIOS | ± 5% |
| | 0 TO 10 OHMS | | 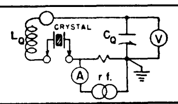 | SUBSTITUTION METHOD | | ± 25% |
| $R_s$ AND $f_r$ (HIGH LEVEL) | 0 TO 100 OHMS AND ABOVE | SPECIAL CIRCUIT ARRANGEMENT | 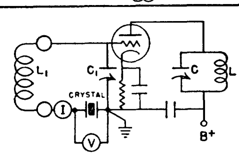 | ADJUST LC FOR MAXIMUM I, AND $E_p$ FOR DESIRED I VALUE. ADJUST $C_1$ FOR MINIMUM V. $R_s = \frac{V}{I}$ | CALIBRATE I AND V. SEE $R_p$ (HIGH LEVEL) | NOT FULLY INVESTIGATED |
| $R_p$ | 5,000 TO 5,000,000 OHMS | "Q" METER WITH LOW $C_Q$ | 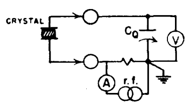 | ADJUST r.f. FOR MAXIMUM V. AT A VALUE HIGHER THAN $f_r$. $R = \frac{Q}{\omega C_Q}$ | V IS MAXIMUM WHEN $C_Q = C_0$ AND FREQUENCY $= f_r + \frac{\Delta f}{2}$ | NOT FULLY INVESTIGATED |

Fig. 6—Tabulation of measurement methods and the accuracies attained.

The values of $R_p$ and $R_s$ may also be derived directly in terms of the $Q$'s observed:

$$R_p = \frac{1.59 \times 10^8 Q_1 Q_2}{f C_{Q1}(Q_1 - Q_2)} \tag{15}$$

$$R_s = R_p' \left[ \frac{(Q_1 - Q_2) C_{Q1}}{Q_1 Q_2 (C_{Q_2} - C_{Q1})} \right]^2 \tag{16}$$

where the symbols are as stated above.[6]

$R_p$ measurements from values of 5 million down to several thousand ohms were readily made with the $Q$ meter using the above formulas. It was found, however, that a direct substitution of calibrated rf resistors in place of the crystal unit (across the $Q$-meter tank) eliminated time-consuming computations, with no sacrifice in accuracy.

Each of a number of coils was resonated at the desired frequency and its $Q_2$ values (see (14)) plotted on semilog paper against rf resistors (on the logarithmic co-ordinate) causing the drop in $Q$. Measurements of $R_p$ at any frequency within a given crystal-unit response were made. At the fixed frequency, the $Q$-meter tank (with crystal unit in shunt) was resonated by tuning the capacitor $C_Q$ to a maximum $Q_2$ indication. Measured $Q_2$ values were converted directly into corresponding $R_p$ values from the resistance ($R_p$) versus $Q_2$ calibration curves. The over-all accuracy (conservatively estimated and tabulated in Fig. 6) is limited by the accuracy to which the rf values of the resistors used for calibration are known, and by the reproducibility of $Q$-meter readings. The inductance and the $Q$ of a specific tuning coil determine the resistance range for greatest accuracy.

To measure the series-resonance frequency, an unshielded coil was resonated in the $Q$ meter at a frequency near that of the crystal unit. The crystal unit was short-circuited and placed near the low-voltage end of the coil. The $Q$-meter frequency was varied until a sharp dip indicated the $f_r$ of the crystal unit.

Measurements of $f_a$, when $C_t = C_0$, were made with the crystal unit in parallel with the $Q$-meter coil. The coil was first resonated at the nominal frequency of the unit. After the insertion of the crystal, the frequency was varied until the $Q$ indicator rose to a maximum. With the crystal unit again removed, the coil was resonated at constant frequency by adjusting $C_Q$. Again the crystal unit was placed in the circuit and the frequency adjusted to a maximum $Q$ indication. These adjustments were repeated until a constant frequency value ($f_a$) was obtained. At this point $C_t = C_0$. For highest precision a final adjustment of $C_Q$ to a maximum $Q$ indication was made at constant frequency. It will be recognized that the $Q$ indication ($Q_2$) yielded the impedance $R_p$ of the crystal unit for this operating point, as previously described.

[6] At high $R_p$ values, $R_p'$ (equation 12) must be used to correct for holder losses.

To measure $f_a$, when $C_t \neq C_0$, the $Q$-meter capacitance was changed from the $C_t = C_0$ setting by the $\Delta C$ required to bring the operating point to the desired frequency within the crystal response, and the frequency was varied to the new $f_a$ indicated by the peaking of the $Q$ indicator. Again the $Q_2$ value yielded the $R_p$ of the crystal unit for this new operating point between $f_a$ and $f_r$.

The $Q$ meter was used for measurements of $R_s$ directly. The crystal units were connected in series with the tank coil for low $R_s$ values (up to 10 ohms), and in parallel with the tank for values higher than 1000 ohms. An rf impedance bridge was found to be more suitable for measurements of $R_s$ from 1 to 1000 ohms.

Values of $R_p$ at crystal-unit voltages approaching those in a Miller- (or Pierce-) type oscillator were measured with a $Q$-meter circuit specifically constructed for the purpose (Fig. 6; see $R_p$ high level). Stable frequency voltage was injected into the $LC$ tank by link-coupling the output of an auxiliary amplifier into a small section of the tank inductance. Sensitive thermoelements and potentiometers were used for current and $Q$ indicators. Care was taken in the measurements to avoid frequency-response shift as the temperature of the crystal varied with the current through it. The technique was modified to permit presetting the voltage levels desired. Since there was no apparent difference in $R_p$ values at high and low voltages (Fig. 7), there seems to be little need for high-voltage measurements, and the procedure is not elaborated upon.

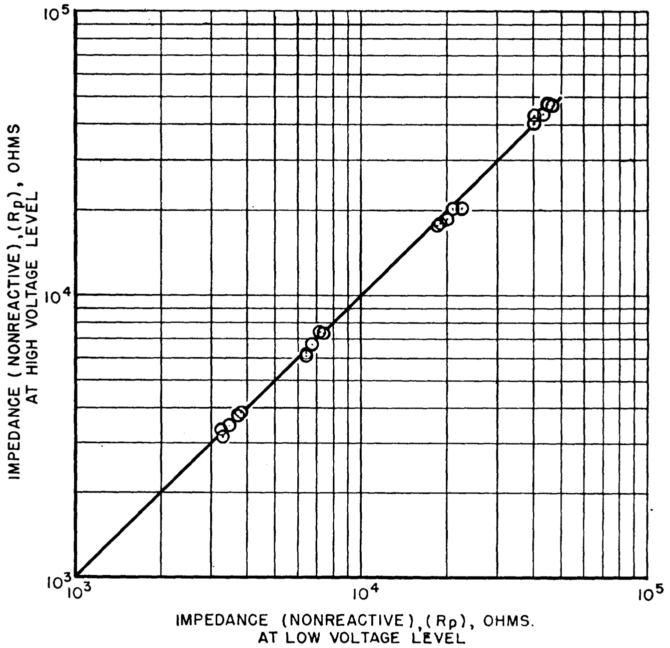


Fig. 7—Correlation between $R_p$ values measured at high and at low rf voltages across the crystal units. Five units were measured with four different values of shunting capacitance.

It should be observed that, when a crystal unit is connected in parallel with an antiresonant circuit tuned approximately to the crystal frequency, there are present two antiresonance peaks of the circuit impedances.[4] The lower peak is not influenced by the frequency response of the crystal unit, and appears at a separation many times the width of $f_a - f_r$. Hence, it does not affect the measurements.

The $Q$ meter was singularly useful in locating and measuring secondary responses. The $Q$-meter tank was tuned to a frequency just below the nominal frequency of the crystal unit. The frequency was then increased continuously, with the crystal unit in parallel with the tank. Voltage dips were observed at $f_r$ points, and peaks at $f_a$ points in the frequency spectrum. Individual responses were closely explored by returning the tank (crystal unit removed) and repeating the sweep of frequency (crystal unit replaced) to determine more exactly the values of $f_r$ and $f_a$. The process of returning the tank and of readjusting the frequency was repeated to a final unchanging frequency.

Tank coils of high inductance were effective in locating $f_a$ points, while low-inductance tank coils were more effective in locating $f_r$'s. For most precise measurements, different coils were used as conditions warranted.

It was found enlightening to plot the relative position of the secondary responses on semilog paper as shown in Fig. 8. For practical purposes, it might be sufficient to interconnect the $R_s$ and $R_p$ points of each response with a straight line, for the curvature involved is negligible relative to the frequency scale employed. This approximation may be justified analytically when considering the variation of $R_e$ within a single response, between $f_r$ and $f_a$.

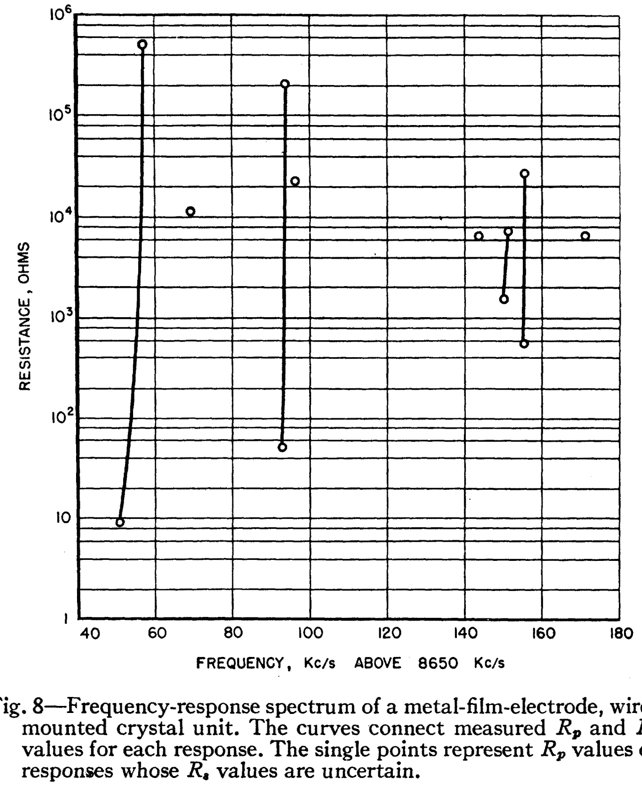


Fig. 8—Frequency-response spectrum of a metal-film-electrode, wire-mounted crystal unit. The curves connect measured $R_p$ and $R_s$ values for each response. The single points represent $R_p$ values of responses whose $R_s$ values are uncertain.

Designating the total series reactance of the equivalent circuit of Fig. 1(a) as

$$X_1 = \omega L_1 - \frac{1}{\omega C_1}, \quad \text{and} \quad X_0 = \frac{1}{\omega C_0},$$

the termination impedance of the unit is

$$Z = X_0 \frac{X_0 R_s + j[R_s^2 + X_1(X_1 + X_0)]}{R_s^2 + (X_1 + X_0)^2}.$$

Then

$$|Z| = X_0 \frac{\{X_0^2 R_s^2 + [R_s^2 + X_1(X_1 + X_0)]^2\}^{1/2}}{R_s^2 + (X_1 + X_0)^2}.$$

The equivalent series values of $R_e$ and $X_e$ are then

$$R_e = \frac{X_0^2 R_s}{R_s^2 + (X_1 + X_0)^2}, \tag{17}$$

and

$$X_e = \frac{X_0[R_s^2 + X_1(X_1 + X_0)]}{R_s^2 + (X_1 + X_0)^2}. \tag{18}$$

For practical purposes, at $f_a$ the reactive component of $Z$ vanishes, and $X_1 + X_0 = 0$; therefore,

$$Z_a \doteq R_p \doteq \frac{X_0^2 R_s}{R_s^2} = \frac{X_0^2}{R_s} \doteq R_e' \tag{19}$$

where $R_e'$ is the value of $R_e$ at $f_a$.

At $f_r$, $X_1$ is zero, and

$$|Z| = X_0 \frac{[X_0^2 R_s^2 + R_s^4]^{1/2}}{R_s^2 + X_0^2} = \frac{X_0 R_s}{(X_0^2 + R_s^2)^{1/2}}.$$

For values $X_0 \gg R_s$, $Z \doteq R_s$. Similarly, at $f_r$, $X_1$ is zero, and, from (17),

$$R_e = \frac{X_0^2 R_s}{R_s^2 + X_0^2} \doteq R_s. \tag{20}$$

It is apparent, therefore, that for responses having series-resistance values considerably lower than $X_0$, plotting $R_e$ versus frequency (Fig. 8) would closely represent a quantitative variation of the parameter of the crystal unit within the limits of $R_s$ and $R_p$. For responses with high series-resistance values, this presentation of a response is correct at the $R_p$ and $R_s$ points only. In the curves shown, the $R_p$ and $R_s$ values representing the top and bottom points of each response are the measured values of these parameters; the intermediate points have qualitative significance only.

The $Q$ meter was used to locate the responses. The $R_p$ and $R_s$ values were then measured with $Q$ meter, twin tee, or rf bridges, depending on the magnitude of the parameter. Some of the relatively small secondary responses ($R_s$ values above 1000 ohms) behaved in a manner that made the measurement of $R_p$ uncertain. Further study of this behavior will be required, and these responses are here represented by a single point of measured $R_s$. Other responses at, and below, the threshold of detectability with the $Q$ meter have been neglected as insignificant in this study.

### *B. Twin-Tee Circuit and Impedance Bridge*

A twin-tee admittance-measuring circuit was used for $R_p$ values of 1000 to 10,000 ohms. Resistance values computed from the admittances obtained were checked often against measurements of rf resistors maintained as standards. Increments of $C_t$ applied across the crystal units (either by varying the internal capacitor of the instrument or by connecting external capacitors across them) were known to high accuracy at the operating frequencies.

It is possible to measure $X_e$ and $R_e$ of a crystal unit directly with the twin tee. However, the relatively limited range of measurable $X_e$ at corresponding $R_e$ values renders the instrument useful only for checking a few points obtained with the $Q$ meter. Its use, therefore, yields little additional information.

An rf impedance bridge was used to measure $R_s$, $R_e$ and $X_s$ values from 1000 down to a few ohms, and $R_e$ values down to 100 ohms. In fact, $R_p$ values as low as 10 ohms were actually measured with 8.7-Mc crystal units. However, the validity of the latter was uncertain.

In measuring $R_s$ and $R_p$ with the bridge, the frequency and resistance arms were varied until a minimum deflection on the null balance indicator was obtained. $R_s$ was measured more rapidly by first determining $f_r$ with the $Q$ meter, as described above. $R_p$ values when $C_t \neq C_0$ were measured with external capacitors connected in shunt with the crystal-unit terminals. $R_e$ and $X_e$ values were obtained at any frequency by adjusting the resistance and reactance arms for a null balance.

The major requirement in the application of the twin tee and rf bridge was a source of stable frequency, adjustable in small increments. Good wave form without frequency modulation was found essential for a sharp null balance.

The equipment shown in the block diagram of Fig. 9 was used for 8.7-Mc crystal-unit measurements. A standard frequency of 100 kc was injected into a frequency multiplier, the products of which were mixed with the output of a continuously adjustable stable-frequency oscillator. The output of the mixer was then amplified to the desired level.

Frequency could be adjusted, measured, and maintained to better than 5 parts in $10^7$ over a period of time required to complete any one measurement. Regular frequency-measuring equipment incorporating a radio receiver as a detector, a stable audio-frequency oscillator to determine the beat frequency between the adjustable oscillator and a harmonic of the standard source, and an oscillograph were used throughout the measurements. A second radio receiver was used as a null indicator for the twin tee and rf bridge.

Special circuits were developed and used to measure independently and directly the values of the series-resonant resistance $R_s$ and series-resonant frequency $f_r$. Fig. 6 lists the methods, accuracies, and range of parameters measured.

## IV. A Complex Crystal Unit

A great difficulty encountered in this investigation was that of locating and segregating a group of quartz-crystal units whose characteristics could be measured, and the results reproduced to an accuracy near that of the measuring equipment. Stability tests of $R_s$, of $R_p$, and of "activity" were made over a period of weeks, and only the most highly stable units were used for measurement.

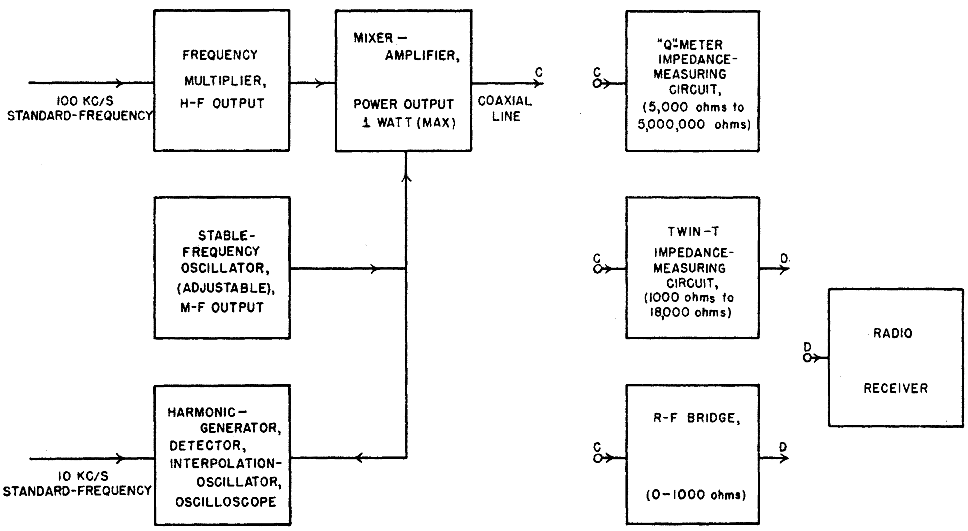


Fig. 9—Block diagram of the apparatus used.

Among those in the select group, there were a few relatively stable with respect to $R_s$ and to "activity," but with $R_p$ (and $\Delta f$) versus $C_t$ characteristics which deviated considerably in slope from the expected 2-to-1 and 1-to-1 ratios. A typical example is shown in Fig. 10.

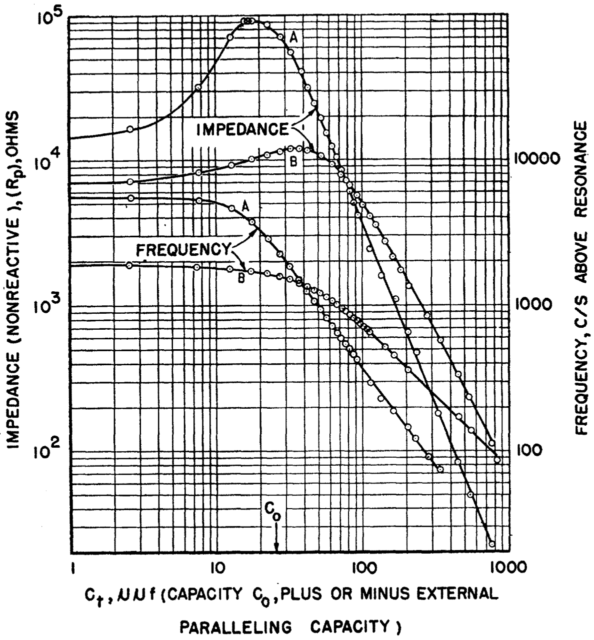


Fig. 10—Electrical characteristics of two interfering responses of a "complex" crystal unit. (a) $f_r$: 8697.87 kc. (b) $f_r$: 8700.40 kc.

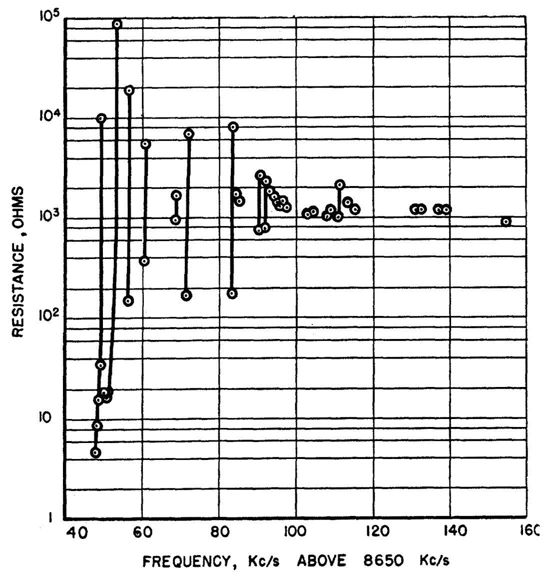


Fig. 11—Frequency-response spectrum of a "complex" crystal unit. The large number of responses should be compared with the relatively few in Fig. 8. The position and magnitude of the antiresonant impedances of the first two responses are indicative of the behavior shown in Fig. 10, and described in the text.

At $C_t$ values between $C_0$ and 75 $\mu\mu$f, the first response ($A$) has higher $R_p$'s than the second; and the crystal should operate at the frequency of the former. Above 75 $\mu\mu$f, the $R_p$ values of the second response are higher; and here the crystal should operate on the second response. This frequency jump from one response to the next was observed in a Miller-type oscillator at the stated $C_t$ value.

It is probable that the presence of many an interfering response will not show up in test oscillators in use at present. This particular one was detected in other measurements: abnormally high $R_s$, and an unusually wide $\Delta f$. The frequency spectrum of this particular crystal unit is shown in Fig. 11. It demonstrates the proximity and the relative values of $R_p$, $R_s$, and $\Delta f$ of all responses; and this frequency spectrum should be compared with the spectrum of the normal crystal unit as shown in Fig. 8.

The role of the second response as an interfering one was again indicated by a decrease in $R_e$ as the frequency was increased from $f_r$. From the minimum, reached several hundred cycles above series resonance, $R_e$ then increased in a more normal manner. This is not intended to indicate a specific manner of behavior of a complex crystal-unit response, but to point out another practical means of exploring such behavior. Further study of this type of crystal should be undertaken as a separate problem, employing methods of measurement described here.

## V. Correlation Between Measured Characteristics and Oscillator Performance of Crystal Units

It has been shown in a number of publications[6,7,8] that the activity of a crystal in an oscillator is a function of the equivalent dynamic resistance $R_p$ ($PI$) of the crystal unit. The higher the $Q$ of a crystal unit, the greater its stability and effectiveness in electric circuits. The relative merits of crystal units may be stated, then, in terms of these parameters.

To verify this, activity, ($I_g$), and $R_p$ measurements were performed on a number of crystal units of varying degrees of stability. Fig. 12 shows thirteen such units with three values of $C_t$ and their corresponding $R_p$'s measured at voltages approximating those across the crystal unit in a Miller-type oscillator. $R_p$ was measured immediately after an $I_g$ measurement to prevent any change in characteristics as a result of handling. To further minimize differences, the activity was later reduced by lowering the oscillator plate voltage, while the $R_p$ measurements were made at the low-voltage levels of the $Q$ meter. These results agree with those in Fig. 12. There is a good correlation between high- and low-activity crystals and their respective $R_p$ values. Moreover, there is good correlation between variation

[7] I. E. Fair, "Piezoelectric crystals in oscillator circuits," *Bell Sys. Tech. Jour.*, vol. 24, pp. 161–216; April, 1945.

[8] M. Boella, "Performance of piezo-oscillators and the influence of the decrement of quartz on the frequency oscillations," Proc. I.R.E., vol. 19, pp. 1252–1274; July, 1931.

in activity of individual crystals and corresponding variation in their $R_p$ values.

Still another correlation exists between the $R_s$ of a crystal unit and its activity in a Miller-type oscillator at various temperatures. Variations in $R_s$ were measured with the crystal unit under test placed in a temperature-controlled cabinet and connected to the impedance bridge through a half-wavelength coaxial cable. Corrections were made for losses in the cable. No difficulties were encountered in the application of the coaxial cable to these measurements.

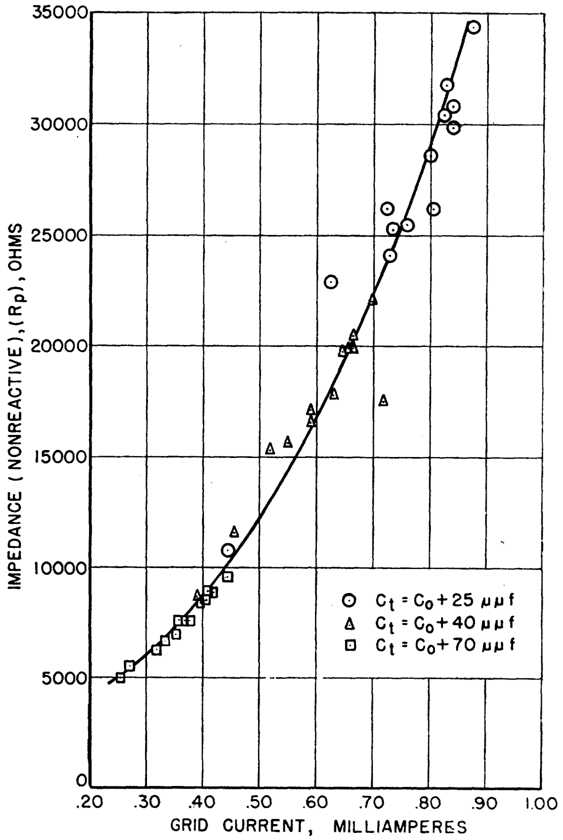


Fig. 12—Correlation between $R_p$ and activity (grid current $I_g$) of thirteen pressure-mounted crystal units.

Since $I_x$ activity is a function of $R_p$, it is also a function of $R_s$ and of $C_t$ (2). Observations were made, therefore, on the effect of temperature on $C_0$. As expected, no detectable variations were found. It may be assumed, then, that the activity variations were caused entirely by changes in $R_s$.

## VI. Additional Observations in Crystal-Unit Measurements

Temperature effects on the relative position of crystal-unit responses and their $R_p$, $R_s$, and $f_a - f_r$ values were measured by the methods described. This type of measurement may be of value in the study of activity dips.

Another graphical presentation of the effect of temperature on the quartz-crystal unit is shown in Fig. 13. In curve A, a relatively high crystal current resulted in a resonance-frequency turning point at an ambient temperature of 3°C. Actually, the high crystal current brought the enclosed crystal plate to a temperature of about 44°C (the nominal turning point), even though the ambient indicating thermometer read 3°C. Curve B shows the resultant shift in turning point to an ambient of 15°C as the crystal assembly was removed from its enclosure and exposed to free ventilation. In curve C,

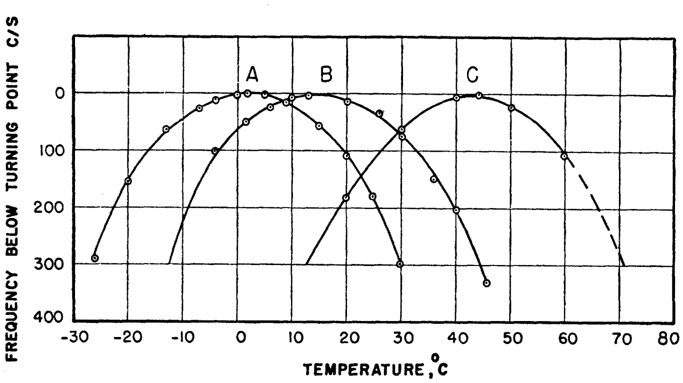


Fig. 13—Effect of operating conditions on the temperature and frequency turning point at resonance of an 8.7-Mc crystal; *BT*-cut, metal-film electrodes, wire-mounted. (A) Crystal in plastic holder, measured with relatively high crystal current. (B) Conditions same as (A), but crystal removed from holder. (C) Crystal in holder again, measured at negligible crystal current.

the crystal current was made negligible, and a full 44°C ambient temperature was necessary to bring the crystal plate to its frequency turning point.

Thus any predetermination of frequency turning point with temperature by a manufacturer or a design engineer must take into consideration at least the approximate amplitude of oscillation expected of the crystal unit and the mechanical design of the crystal-plate holder and electrodes, insofar as heat dissipation is concerned. This is in keeping with the observation that the graphical curves suggested for use in design work should be accomplished by temperature data for a more complete expression of the characteristics of a quartz-crystal unit.

## VII. Conclusion

It was shown that comprehensive data on electrical characteristics of quartz-crystal units may be obtained with rf bridges and $Q$ meters and a source of constant cw frequency. Electrical characteristics of fundamental or of secondary responses may be measured equally well by the methods described.

Graphical presentation of measured parameters as straight-line functions on log-log co-ordinate paper was suggested as particularly suitable for design purposes. Examples of crystal behavior were given to demonstrate this presentation.